Encapsulation of Nickel Nanoparticles in Carbon Obtained by the Sonochemical Decomposition of $Ni(C_8H_{12})_2$

Yuri Koltypin,[†] Asuncion Fernandez,[‡] T. Cristina Rojas,[‡] Juan Campora,[§] Pilar Palma,[§] Ruslan Prozorov,[||] and Aharon Gedanken*,[†]

Departments of Chemistry and of Physics, Bar-Ilan University, Ramat-Gan, Israel, 52900, and Instituto de Ciencia de Materiales de Sevilla, Insituto de Investigaciones Quamicas, and Dpto. Quimica Inorganica, Centro de Investigaciones Cientificas Isla de la Cartuja, Avda, Americo Vespucio s/n, 41092-Sevilla, Spain

Received December 7, 1998. Revised Manuscript Received February 22, 1999

A new precursor for the sonochemical preparation of amorphous nickel, Ni(cyclooctadiene)$_2$, yielded relatively large (200 nm) amorphous nanoparticles composed of nickel and carbon atoms. Small nickel particles were dispersed all over the particle. When these particles were heated slightly above their crystallization temperature, much smaller particles (5 nm) of encapsulated crystalline nickel in amorphous carbon were obtained. The XPS spectrum reveals that the crystallization process is also accompanied by the reduction of the surface Ni^{2+} ions by the amorphous carbon atoms. The DSC measurements substantiate this assumption.

Introduction

The use of ultrasound radiation for the preparation of nanophased amorphous metals was first demonstrated by Suslick and co-workers[1,2] The irradiation of $Fe(CO)_5$ as a neat liquid or in Decalin solution[2] has led to the formation of 10−20-nm particles of amorphous iron. Suslick has extended his studies[3] and prepared nanophased amorphous cobalt as well. Following in Suslick's steps we have reported on the synthesis of amorphous nickel where the starting material was $Ni(CO)_4$,[4] which is known as a hazardous material. Our synthetic efforts also included the preparation of amorphous transition metal oxides (Fe_2O_3,[5] Cr_2O_3 and Mn_2O_3,[6] and Mo_2O_5[7]), transition metal nitrides,[8] and ferrites.[9] Nonmagnetic metals[10,11] have also been synthesized by this technique. Surprising results were obtained when the precursor for the preparation of Pd, $Pd_2(DBA)_3$ (DBA, dibenzoil acetone) was sonicated in a mesitylene solution and yielded a 3−5-nm amorphous metallic Pd core surrounded by a 3−5-nm ring of carbon atoms.[10]

Rao and co-workers have encapsulated Fe, Co, and Ni in graphite using the arc evaporation method.[12] They have investigated two regions: the first, the cathodic stub, showed metallic particles (10−40 nm) present in the voids of the carbon onions, and the second, in the soot where small carbon-coated metallic particles in the 2−15-nm range, were found. The iron particles in the stub were ferromagnetic, while those in the soot, superparamagnetic.[12] The arc evaporation of graphite electrodes, with an anode filled with Fe_2O_3, has yielded metallic iron,[13] as well as iron carbides wrapped within onions in the cathodic deposits. Rao and co-workers have recently applied gas-phase pyrolysis of metallocenes and mixture with benzene[14] and acetylene[15] and obtained carbon nanotubes and metal-filled onion-like structures.[14] In the latter case[15] they also obtained single-walled carbon nanotubes.

A recent paper discussing the encapsulation of magnetic (nickel and cobalt) particles in graphite, has used the tungsten arc technique, where an electric arc

[†] Department of Chemistry, Bar-Ilan University.
[‡] Instituto de Ciencia de Materiales de Sevilla and Dpto. Quimica Inorganica, Centro de Investigaciones Cientificas Isla de la Cartuja.
[§] Insituto de Investigaciones Quamicas and Dpto. Quimica Inorganica, Centro de Investigaciones Cientificas Isla de la Cartuja.
[||] Department of Physics, Bar-Ilan University.

(1) Suslick, K. S.; Choe, S. B.; Cichowlas, A. A.; Grinstaff, M. W. *Nature* **1991**, *353*, 414.
(2) Grinstaff, M. W. ; Cichowlas, A. A.; Choe, S. B.; Suslick, K. S. *Ultrasonics* **1992**, *30*, 168.
(3) Suslick, K. S.; Fang, M.; Hyeon, T.; Cichowlas, A. A. *Molecularly Designed Nanostructured Materials*; MRS Symp. Proc. Vol 351; Gonsalves, K. E., Chow, G. M., Xiao, T. O., Cammarata, R. C., Eds., Materials Research Society: Pittsburgh, 1994; pp. 443−448.
(4) Koltypin, Yu.; Katabi, G.; Prozorov, R.; Gedanken, A. *J. Non-Cryst. Solids*, **1996**, *201*, 159.
(5) Cao, X.; Prozorov, R.; Koltypin, Yu.; Kataby, G.; Gedanken, A. *J. Mater. Res.* **1997**, *12*, 402.
(6) Dhas, N. A.; Gedanken, A. *Chem. Mater.* **1997**, *9*, 3159.
(7) Dhas, N. A.; Gedanken, A. *J. Phys. Chem.* **1997**, *101*, 9495.
(8) Koltypin, Yu.; Cao, X.; Prozorov, R; Balogh, J.; Kaptas, D.; Gedanken, A. *J. Mater. Chem.* **1997**, *7*, 2453.
(9) Shafi, K. V. P. M.; Koltypin, Yu.; Gedanken, A. *J. Phys. Chem.* **1997**, *101*, 6409.
(10) Dhas, N. A.; Cohen, H.; Gedanken, A. *J. Phys. Chem. B* **1997**, *101*, 6834.
(11) Dahs, N. A.; Raj, C. P.; Gedanken, A. *Chem. Mater.* **1998**, *10*, 1446.
(12) Seshadri, R.; Sen, R.; Subbanna, G. N.; Kannan, K. R.; Rao, C. N. R. *Chem. Phys. Lett.* **1994**, *231*, 308.
(13) Saito, Y.; Yoshikawa, T.; Okuda, M.; Fujimoto, N.; Yamamura, S.; Wakoh, K.; Sumiyama, K.; Suzuki, K.; Kasuya, A.; Nishina, Y. *Chem. Phys. Letts.* **1993**, *212*, 379.
(14) Sen, R.; Govindaraj, A.; Rao, C. N. R. *Chem. Phys. Lett.* **1997**, *267*, 276.
(15) Satishcumar, B. C.; Govindaraj, A.; Sen, R.; Rao, C. N. R. *Chem. Phys. Lett.* **1998**, *293*, 47.
(16) Host, J. J.; Block, J. A.; Pravin, K.; Dravid, V. P.; Alpers, J. L.; Sezen, T.; LaDuca, R. *J. Appl. Phys.* **1998**, *83*, 793.

10.1021/cm981111o CCC: $18.00
Published on Web 04/17/1999

coevaporates metal and carbon from a liquid metal pool.[16] The paper presents a comprehensive review of the various methods for the preparation of metals encapsulated in carbon. Powder XRD profiles show peaks associated with single phase of fcc cobalt or nickel.

The aim of the present study is to find a "healthier" precursor for the preparation of amorphous metallic nickel. We have sonicated a 0.02 M solution of $Ni(COD)_2$ (COD, cyclooctadiene) in toluene. The as-prepared product contained 49.5% carbon, 1.2% hydrogen, and 49% nickel. The product was formed in the amorphous state. This manuscript will outline the structure and physical properties of the as-prepared and the corresponding crystalline material. Unlike Rao and co-workers,[12,14,15] carbon nanotubes were not obtained as products of the sonication process.

Experimental Section

$Ni(COD)_2$ was synthesized according to a known procedure.[17] The product was crystallized twice from THF and was free of NaCl. Although the sensitivity of the $Ni(COD)_2$ to air would have allowed us to work in air for a short period (10 min), we have avoided the air presence by handling the preparation of the solution in a glovebox. The $Ni(COD)_2$ toluene solution was sonicated (Sonics and Materials, VC-600, 20 kHz, 100W/cm^2) for 5 h under an argon pressure of 1.5 atm. The sonication cell was immersed in an acetone−dry ice bath, yielding a temperature of ∼0 °C inside the sonication cell. At the end of the irradiation, the resulting solid product was washed thoroughly with dry pentane and centrifuged. This process was repeated three times. The product was then dried under vacuum and kept in a glovebox (<2 ppm O_2). Toluene (99.8% anhydrous, Aldrich) was used after its purification with molecular sieves.

TEM (Transmission Electron Microscopy) measurements were carried out both in Israel (low resolution) and Spain (higher resolution). The instrument located in Israel is a JEOL-JEM 100SX electron microscope. The instrument located in Spain is a Philips CM200 microscope operated at 200 kV. The powdered samples were dispersed in hexane or ethanol by sonication and dropped on a conventional carbon-coated copper grid. Magnetization loops were measured at room temperature, using a VSM, Oxford Instrument Vibrating Sample Magnetometer.

The DSC (Differential Scanning Calorimetry) spectra were recorded using a Mettler DSC 25 (TC15 TA controller) instrument in the temperature range of 25−500 °C. Powder X-ray diffractograms were recorded on Rigaku X-ray diffractometer (Cu Kα radiation, $\lambda = 0.15418$ nm). Surface area (BET method) measurements were carried out using a Micromeritics-Gemini surface area analyzer, employing nitrogen gas adsorption. Toluene (99.8% anhydrous, Aldrich) was used after its purification with molecular sieves. X-ray photoelectron spectroscopy analysis was carried out in a VG210 ESCALAB instrument operated with Al Kα radiation in the $\Delta E = 50$ eV constant mode.

Elemental analysis of C, H, S, and N was carried out on an Eager 200 CE Instruments EA 1110 Elemental Analyzer. The as-prepared material (named Ni/C) contains 50.0% carbon and 1.2% H. A similar composition was measured for the crystallized material (named Ni/C 500): 53% carbon and 1.3% hydrogen.

Results

The amorphous nature of the product is demonstrated in Figure 1, which depicts the XRD of the as-prepared (a) and the crystallized sample (b). To convert the amorphous material into the crystalline state, the sample was heated at 500 °C for 20 h under a flow of pure argon (<2 ppm impurities). The XRD pattern of the crystalline material fits the fcc structure of γ-nickel. No evidence for the existence of nickel oxide, nickel carbide, or any crystalline phase of the carbon is detected. The broad peaks are indicative of the small particle size of the crystalline material. The application of the Debey−Scherrer equation for the analysis of the line widths yielded a 3.2-nm size for the nanocrystalline product. It is worth mentioning that the chemical analysis of the crystalline material revealed 53% carbon and 1.3% hydrogen. The atomic ratio of carbon:hydrogen is about 3.5:1. This ratio is different from the carbon: hydrogen ratio in the precursor, 1:1.5.

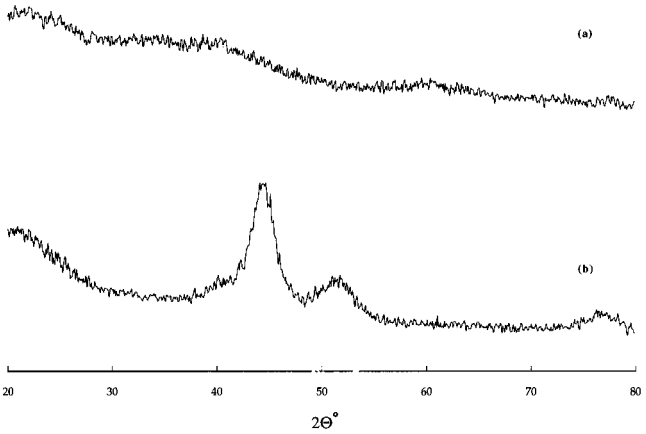

Figure 1. (a) XRD spectra of the as-prepared (Ni/C) material, and (b) of the crystallized material (Ni/C-500).

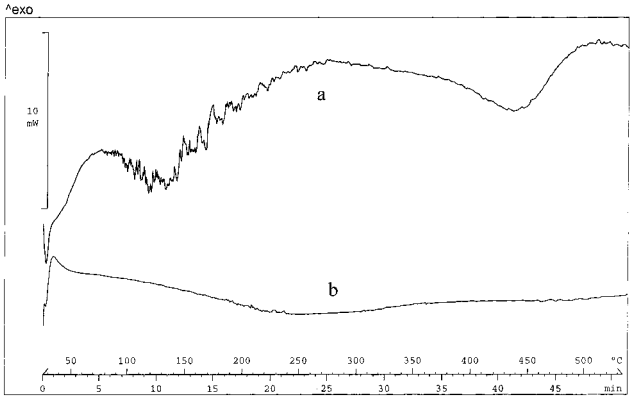

Figure 2. (a) The DSC spectrum of the as-prepared material (heating rate is 10 °C/min) and (b) a second DSC run of the sample presented in part a, after it has been cooled to room temperature under argon (heating rate is 10 °C/min).

The DSC spectrum of the as-prepared product is presented in Figure 2. It shows (part a) an endothermic peak at 130 °C, which is explained as the desorption of solvent molecules and the precursor's ligands from the surface of the product particles. This endothermic peak is followed by a very broad exothermic band peaked at 280 °C. We assign this peak to the crystallization of the amorphous product. The width of this peak has to do with the wide distribution of the particle sizes of the product. Another endothermic peak is detected at 440 °C. Both peaks did not show up when the heated sample was cooled to room temperature under argon and the DSC was remeasured (part b). The 440 °C endothermic

(17) Colquhoun, M. M.; Holton, J.; Thompson, D. J.; Twiggs, M. V. *New Pathways for Organic Synthesis. Practical Applications of Transition Metals*; Plenum Press: New York, 1984;, p 389.

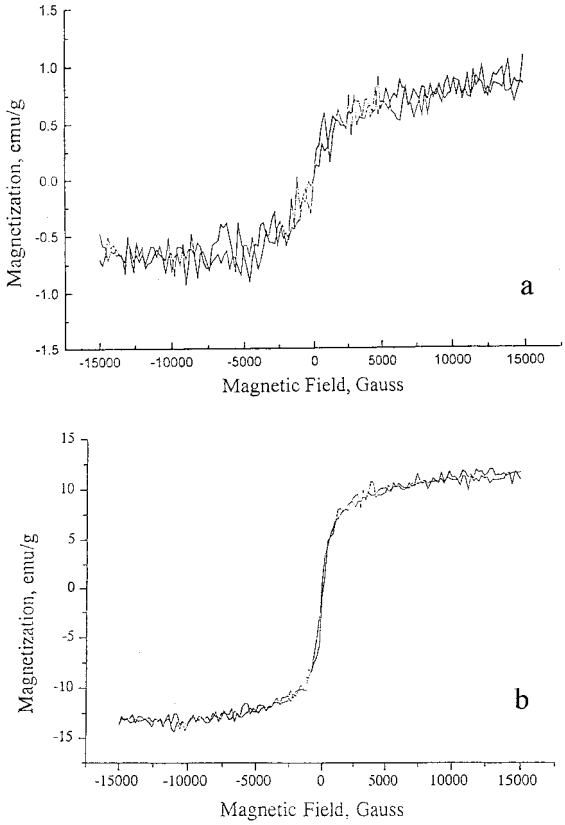

Figure 3. (a) Room-temperature magnetization loop of the as-prepared material (Ni/C) and (b) room-temperature magnetization loop of the crystallized material (Ni/C-500).

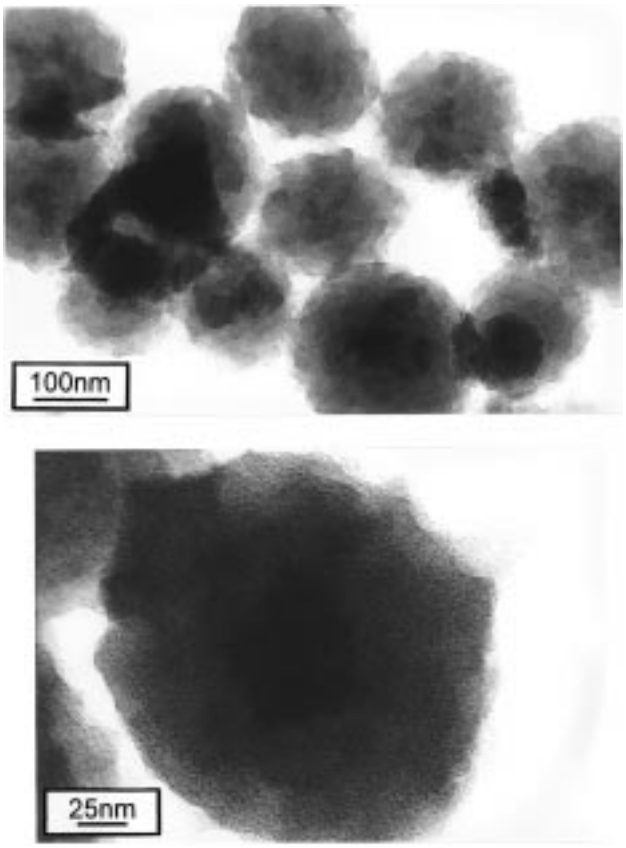

Figure 4. TEM images of the as-prepared material (Ni/C).

peak is attributed to the reduction of the Ni^{2+} ions by the carbon atoms. The reaction is endothermic at 25 °C, as well as at 440 °C. The $\Delta G°$ at 25 °C is positive. Due to its positive $\Delta S°$, its free energy changes sign and the reaction becomes spontaneous at elevated temperatures. The disappearance of the peaks at 280 and 440 °C in the second DSC run (Figure 2b) substantiates this interpretation. The TEM, EDX, and the XPS measurements, which help to identify and characterize the products, further substantiate this interpretation.

In Figure 3, we present the room-temperature magnetization loops of the amorphous (part a) and crystalline (part b) materials. A very small magnetization was found for the amorphous nickel, on the range of 1 emu/g of nickel. On the other hand, when the material was crystallized a value of about 25 emu/g of nickel was measured. For bulk Nickel, the corresponding value is 60 emu/g.[4] The magnetization did not reach saturation at 15 kG, and did not show hysteresis. This is a typical behavior of a superparamagnetic material. We believe that the mean size of the coherently diffracting domains, 2−3 mm, obtained by the XRD diffraction, is reflecting the size of the individual single domain particles. The TEM images on the other hand depict the aggregated particle composed of many small singlets. The drastic change in the magnetization values upon crystallization is explained as follows. The as-prepared amorphous nickel is dispersed in carbon, so it is considered as a solid solution of nickel atoms in carbon. Therefore the magnetization is extremely weak, and there is no hysteresis (because, physically, the magnetization is due to separate nickel atoms). During crystallization these atoms form larger nickel particles with exchange interactions inside each nanoparticle.

Two TEM pictures are presented in Figure 4 depicting the images of the as-prepared nickel particles. The typical diameters of the particles are about 100−200 nm. The surface area measured for the as-prepared particles is 40 m^2/g. The electron diffraction pattern of the as-prepared material reveals diffuse rings typical for the amorphous nature of the material. Figure 5 depicts two TEM images of the as-prepared material heated in an inert gas atmosphere to 500 °C, a temperature above its crystallization temperature. It is clear from the TEM pictures that the as-prepared material has undergone a morphological transformation upon heating. This is reflected in the formation of 5−20-nm-sized nickel particles that appear embedded in amorphous carbon. This morphological change is also reflected in a dramatic increase in the surface area from the above-mentioned 40 m^2/g for the as-prepared material to 326 m^2/g for the heated material. The same phenomenon is observed when the as-prepared sample was heated "in situ" at the electron microscope. The electron diffraction of the heated material depicted in Figure 5 (see inset) clearly shows the diffraction pattern of crystalline nickel.

The TEM pictures of the "in situ" heated material are depicted in Figure 6. It can be observed that some particles show in the center a higher concentration of lager nickel particles which has been confirmed by EDX analysis.

Figure 7 depicts the XPS spectra of C 1s, and Ni 2p, as well as the NiL3VV Auger spectrum. These spectra are presented for the as-prepared material and for the

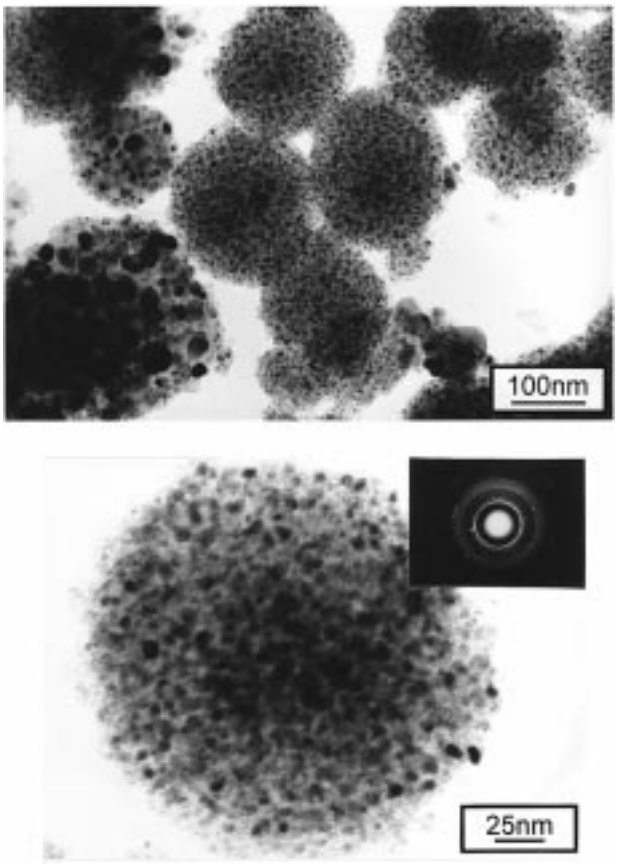

Figure 5. TEM images of the crystallized material (Ni/C-500), the inset depicts the microdiffraction pattern of the crystallized material.

heated sample. The main Ni peaks in the as-prepared material are the Ni $2p_{3/2}$ peak at 855.7, and the Ni $2p_{3/2}$ at 873.4 eV, as well as their corresponding shake-up resonances at 861.4 and 880.0 eV. These peaks are assigned to oxidized nickel in a dispersed phase.[18] The XPS technique probes mostly the surface of the particles, and it is expected that a highly dispersed nickel phase mixed with carbon and exposed to air will appear oxidized at the surface. On the other hand, the heating of the sample reveals a new peak at 853.0 eV, in addition to the $2p_{3/2}$ 855.7 eV peak and the shake-up resonance at 861.4 eV. This additional peak and its $2p_{1/2}$ spin−orbit component at 870.4 eV fit very well the previously reported results for zerovalent metallic nickel.[19] Same results can be concluded from the Auger peaks. The detection of metallic nickel at the surface of the sample indicates clearly the reduction of Ni^{n+} species when the original sample is heated in argon at 500 °C. The particles may also be covered by carbon atoms, protecting them from further oxidation. The mechanism by which the encapsulated crystallized Ni^0 is obtained will be discussed. It may be associated with the above-mentioned endothermic DSC peak observed at 440 °C.

The C 1s spectra that were used for calibration at 284.6 eV carbonate species and other C−O bonds should

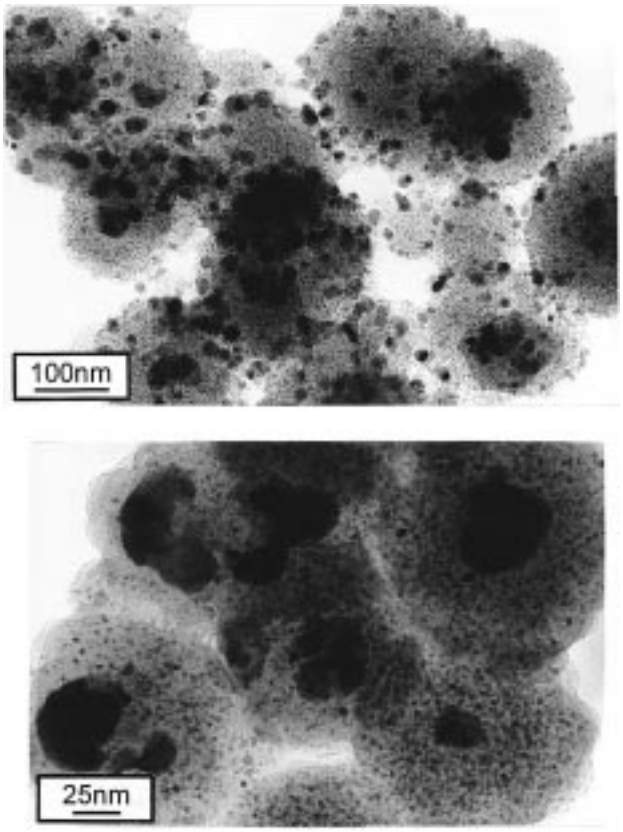

Figure 6. TEM images of the samples heated "in situ" at the electron microscope.

appear around 290 eV.[20] No evidence of these species has been observed in our XPS data. In addition a very small bump around 290 eV on the C 1s spectra is a characteristic of a graphite-like carbon.[21]

Discussion

The sonochemical decomposition of the $Ni(COD)_2$ has led to the formation of a nickel core encapsulated in an envelope of highly dispersed nickel in amorphous carbon. This unusual dissociation process has to do with the extreme conditions, which occur upon the collapse of the cavitaion bubble.[1] Unlike the sonochemical decomposition of the transition metal carbonyls, which leads to the formation of nanophased amorphous metal (while the CO is released to the gas flowing above the reaction mixture),[1−6] the COD ligand is adsorbed on the surface of the freshly formed nickel particle. It further undergoes dissociation, leading to the formation of the carbon envelope. Similar results have recently been reported by Nuzzo's group. In their experiment, a ligand, hexafluoroacetylacetonate (hfac), was transferred at low temperature to a copper surface from a $Pd(hfac)_2$ adsorbed onto the copper surface. Upon annealing of the surface, the surface-bound hfac ligands decomposed, yielding a "possibly graphitic" [22] carbon residue on the copper surface. A similar decomposition pattern occurred when a $Pd_2(DBA)_3$ solution was ultrasonically

(18) Kim, K. S.; Davis, R. E. *J. Electron Spectrosc. Relat. Phenom.* **1972**, *1*, 252.
(19) Briggs, D., Seah, M. P., Eds. *Practical Surface Analysis by Auger and X-ray Photoelectron Spectroscopy*; John Wiley & Sons: New York, 1983.
(20) Gonzales-Elipe, A. R.; Espinos, J. P.; Fernandez, A.; Munuera, G. *Appl. Surf. Sci.* **1990**, *45*, 103.
(21) Caballero, A.; Espinos, J. P.; Fernandez, A.; Soriano, L.; Gonzalez-Flipe, A. R. *Surf. Sci.* **1996**, *364*, 253.
(22) Bent, B. E.; Nuzzo, R. G.; Dubois, L. H. *J. Am. Chem. Soc.* **1989**, *11*, 1634.

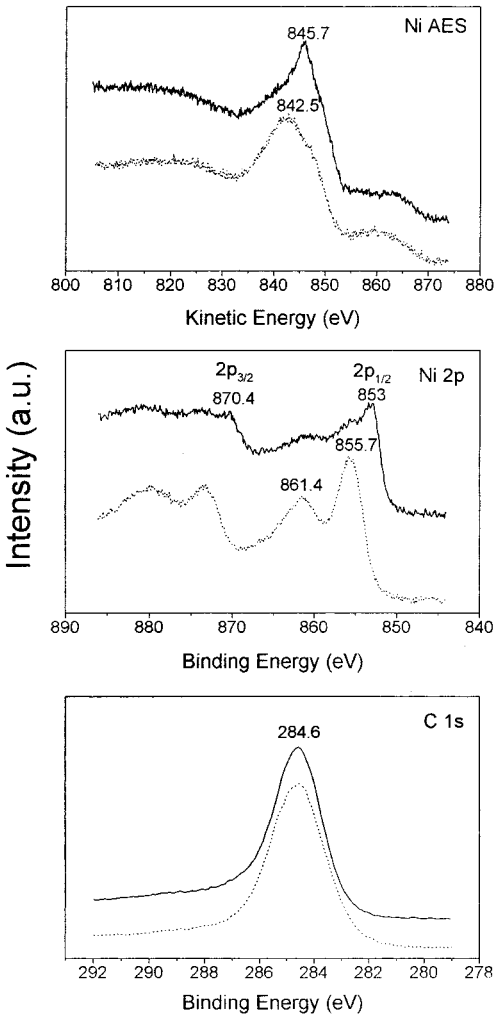

Figure 7. The XPS of the Ni 2p, C 1s, and Ni L3VV Auger spectra of the as-prepared (Ni/C, dotted line) and the crystallized (Ni/C-500, solid line) materials.

irradiated, yielding Pd encapsulated in a carbon envelope.[10] Nuzzo[22] has suggested that defect sites can accelerate the rates of such reactions when an adsorbate undergoes dissociation reactions. In the case of the bubble collapse, this might be even further emphasized, because the formed in situ particle is amorphous and enriched in defect sites. Its enormous surface area would further enhance the decomposition of the ligand.

Another unique phenomenon that we have experienced in this study is the dramatic change that the as-prepared material undergoes upon its crystallization, leading to an 8-fold increase in its surface area. This change is observed in the TEM in the crumbling of the 200-nm particles into smaller particles. Since it involves the presence of carbon atoms, it immediately evokes the possibility of an exfoliation process that graphite undergoes.[23,24] However, despite a few similarities, the main difference is the particle nature in the current case versus the graphitic layered structure, in the exfoliation process. We associate the crumbling of the 200-nm particle with the crystallization process that triggers the entire process. We will also argue that this crumbling starts at the surface and continues toward the center. The nickel centers at the outer surface undergo a volume change upon crystallization. Due to the attractive forces with the surrounding carbon atoms, the amorphous carbon envelops this center. The amorphous carbon is described as "streaming" toward and around these nickel centers, forming small nuclei. These nucleation centers continue to grow toward the center of the 200-nm particle, leaving the crumbled particles crystallized.

We have also detected the reduction of the dispersed nickel ions to the metallic nickel as is evident from the XPS spectra. The reducing agent is the amorphous carbon, and the process occurs at 440 °C, as deducted from the endothermic peak at the same temperature in the DSC spectrum.

Conclusion

This research work has demonstrated again that ultrasound radiation can be used for the in situ preparation of amorphous carbon-activated nickel nanoparticles. Nickel on the surface of the as-prepared particle is oxidized (Ni^{2+} and Ni^{3+}). When the particle is heated to 500 °C it undergoes a number of changes: (1) a chemical reaction, in which Ni^{2+} and Ni^{3+} are reduced to Ni^0 by the amorphous carbon; (2) the crystallization of the amorphous nickel; (3) a morphological change where the 100−150-nm-sized particle is broken to 5−20 nm; and (4) a dramatic change in the magnetization of the material is detected.

Acknowledgment. A. Gedanken thanks the Ministry of Science and Technology for an Indo-Israeli Grant in Material Science. Yu. Koltypin thanks the Ministry of Absorption, the Center for Absorption in Science for its financial help. The authors from ICMSE, Spain, thank the DGES for financial support (Project Number PB96-0863-C02-02). We also thank Dr. Shifra Hochberg for editorial assistance. This research was also financially supported by NEDO International Joint Research Grant.

CM981111O

(23) Chung, D. D. L. *J. Mater. Sci.* **1987**, *22*, 4190.
(24) Dowell, M. B.; Howard, R. A. *Carbon* **1986**, *24*, 311.